CIVIL ENGINEERING JOURNAL

Article no. 40

THE CIVIL ENGINEERING JOURNAL 4-2023

# ANALYSIS AND OPTIMIZATION OF WIND RESISTANCE PARAMETERS FOR LATTICE-TYPE HIGH-MODULUS SUPPORTS BASED ON THE OPTIMAL CRITERIA METHOD

*Qingyu Sui, Quansheng Sun, Jianxi Yang and Shijie Wang*

*School of Civil Engineering and Transportation, Northeast Forestry University, Harbin 150040, China; sunquansheng@nefu.edu.cn*

## ABSTRACT

Lattice high-molded support can generally be used for cast-in-place support for bridges, but for more than 50 meters of lattice high support, due to the wind, load and other factors, due to the support length and slenderness of the relatively large, relatively light and flexible structure and other characteristics of the role of the wind load is very sensitive. When the lattice high-molded stent construction is used in the typhoon area, it is easy to be damaged by the typhoon, and the structural design of the lattice high-molded stent and the construction of that technology are facing great challenges. In this paper, based on the new construction of a special bridge in Fujian, finite element analysis of four-legged and six-legged lattice bracing is carried out by ANSYS, and the effects of steel pipe diameter, number of columns, longitudinal and transversal spacing of bracing, and diagonal bracing structural parameters on structural performance are analyzed by using the coefficients of buckling stability and the coefficients of critical loading. The results of the study show that the main design variable for displacement sensitivity is the diameter of vertical rod; the main design variable for stress sensitivity is the diameter of diagonal rod; the main design variable for overall stability sensitivity is the diameter of diagonal rod; and the main design variable for overall stability sensitivity of total volume is the diameter of diagonal rod. And the optimal wind resistance parameters are: 4 lattice high-braced columns are selected, the section length should be controlled within 15m, and the total height should not be more than 70m, and the spacing of the columns is controlled between 7m and 8m. This study proposes a set of optimized design process method for wind-resistant lattice structure under the constraints of stiffness, strength and critical load factor, which improves the economy and ensures the reasonableness of the design, and can be used for the design of high-modular lattice bracket in typhoon area.

## KEYWORDS

Lattice bracing, Wind effects, Optimality criterion method, Nonlinear analysis

## INTRODUCTION

With the rapid development of China's economy and technology, coupled with the implementation of policies such as reform and opening up, and the Belt and Road Initiative, a large number of large bridges spanning rivers, seas, canyons, lakes, and existing roads have been successively completed. This has ushered in a golden period of vigorous development in the country's transportation infrastructure, with constantly refreshed lists of bridge spans. As bridges gradually move towards large spans, wind damage has also gradually come into view for engineers [1]. In recent years, with global climate warming and the frequent occurrence of extreme weather, the frequency of natural disasters has been increasing year by year. Due to geographical characteristics, coastal areas in China become the main targets of typhoons. Statistics show that Guangdong, Fujian, Zhejiang, and other regions are affected by typhoons about 7.2 times each year.

Currently, in China, large-span continuous concrete bridges are mainly constructed using the scaffolding method. Common types of scaffolding include fastener-type steel pipe scaffolding, bowl-type steel pipe scaffolding, portal scaffolding, among which the steel pipe truss modular support system has proven its practicality and effectiveness in practice, playing a crucial role in large-span bridge construction projects [2]~[6].

In recent years, the grid-type high-modulus support system has been widely used due to its convenient assembly and strong load-bearing capacity. Due to its towering, flexible structural form, as well as its light weight and low damping characteristics, the grid-type high-modulus support system has strong sensitivity to wind. Large-span bridges are usually located in areas with fast winds such as rivers, seas, and canyons, and the construction area occupied by scaffolding is usually extensive with high wind resistance. Therefore, it is necessary to carry out experimental research on the wind-resistant design optimization of scaffolding. During the construction of bridges, scaffolding not only serves to provide a working surface but also provides structural bearing capacity when the early concrete strength has not formed. The design and use of scaffolding determine the progress and safety of engineering projects. The wind stability of scaffolding has attracted the attention of many scholars at home and abroad.

During bridge construction, supports not only provide a working surface but also provide structural load-bearing capacity in the early stages before the concrete strength has fully developed. The design and use of supports determine the progress and safety of engineering projects. Support wind stability has attracted the attention of many domestic and foreign scholars [7]~[13]. In 2006, Xiu Lei [14] used simplified formulas and random vibration theory to simplify the wind-induced response of lattice-type tower structures into algebraic calculations. Using a first-order generalized load spectrum analytical model, they proposed a simplified calculation formula for the downwind wind-induced response of lattice-type tower structures. In 2022, Yang Wen [15] conducted nonlinear analysis research on the yielding mechanism of lattice-type steel-concrete tower structures based on static experiments of four ball-joint node models simulated using Abaqus finite element simulation software. The research results showed that node failure is mainly caused by strength failure and compressive member instability, and the difference in node plate thickness has a more significant impact on the bearing capacity of ball-joint nodes, while changes in the thickness ratio of the enclosure diameter have less impact on the bearing capacity of ball-joint nodes. In 2023, Jeddi Ashkan B [16] and others used the Kalman filter method to study the drag coefficient and gust response factor of double-loop lattice-type transmission towers, accurately estimating the impact of extreme wind-induced loads on lattice-type structures. Based on the aerodynamic characteristics and wind tunnel tests, an optimized Kalman filter model was proposed to integrate measurements from multiple sensors of the same and different types implemented in wind tunnel experiments. This approach, combined with optimization techniques, provided estimates of the wind load parameters of interest with high spatial resolution and accuracy in measuring response.

This study utilizes the ANSYS finite element simulation program to establish lattice-type high modulus supports under wind load, and, in combination with MATLAB programming software, for secondary development to improve structural optimization accuracy. The modified optimal criteria method is used to correct the stiffness, strength, and critical load factor constraint formulas, proposing a wind-resistant optimization design process for lattice-type high modulus supports based on the modified optimal rule."

CIVIL ENGINEERING JOURNAL

Article no. 40

THE CIVIL ENGINEERING JOURNAL 4-2023

# ESTABLISHMENT OF FINITE ELEMENT ANALYSIS MODEL FOR LATTICE-TYPE HIGH MODULUS SUPPORT

## Project overview

*Tab. 1 - Support system material specifications（unit：mm）*

| Number | Foundation type | Column steel pipe | Flat-coupled steel pipe | Diagonal brace steel pipe | Steel |
|---|---|---|---|---|---|
| D0~9# | Reinforced concrete strip foundation | Φ720×14 | Φ400×8 | Φ400×8 | Q345 |
| D9~19# | Bored pile foundation | Φ1200×14 | Φ720×14 | Φ400×8 | Q345 |

The bridge spans are configured as follows: 4 spans of 40 meters each, 4 spans of 40 meters each, 6 spans of 40 meters each, 5 spans of 40 meters each, and 4 spans of 32 meters each, with a total length of 888 meters. This study is based on a representative bridge, and the strait where the bridge is located can experience gusty winds exceeding 10 on the Beaufort scale in the absence of typhoon effects. Adequate clearance height is not guaranteed to ensure safe navigation. During the construction of the supports, the support height exceeds 15 meters, making it a high-modulus support construction.

## Finite element model establishment

According to the design drawings, three-dimensional spatial computational models of four-legged lattice-type high modulus supports and six-legged lattice-type high modulus supports were established using finite element analysis software ANSYS for structural simulation analysis. The four-legged lattice-type high modulus support has a height of 41.7 meters and is divided into 722 nodes and 756 computational elements. The six-legged lattice-type high modulus support has a height of 52.4 meters and is divided into 1439 nodes and 524 elements. The finite element models are established as shown in Figure 1 and 2, with the X-direction representing the longitudinal bridge direction, and the Y-direction representing the transverse bridge direction.

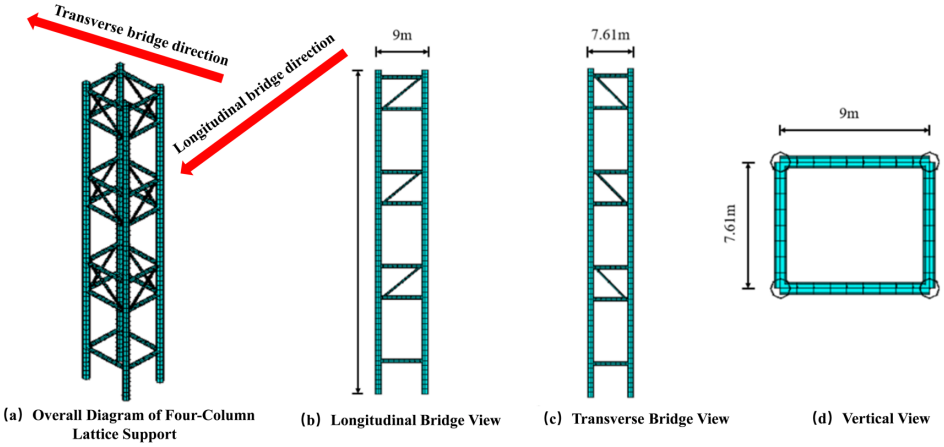


*Fig. 1 - Four-Legged Lattice Support*

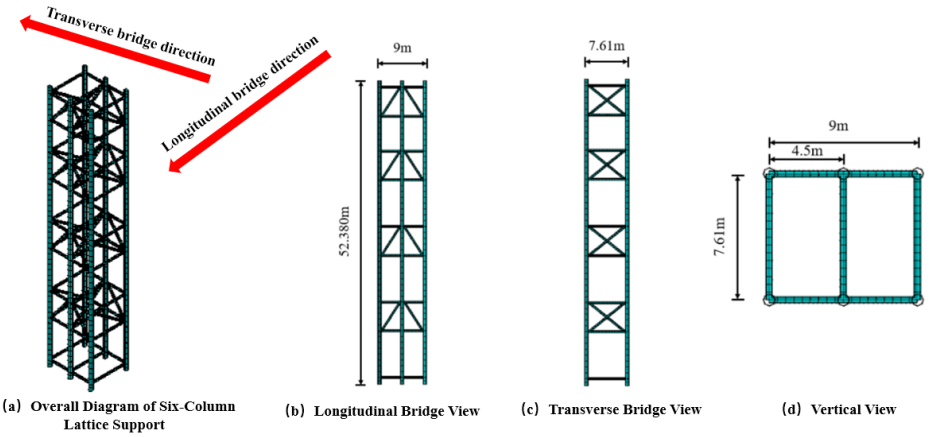


*Fig. 2 - Six-Legged Lattice Support*

## Finite element model structural optimization

### *Node displacement optimization*

In the process of structural optimization design for high-modulus supports under wind loads, displacement deformation is the primary manifestation of the structural stress state. Displacement constraint factors need to be considered in the structural optimization design. By controlling node movements, the deformation of the structure gradually decreases, ultimately meeting the constraints on structural stiffness.

In the structural shape optimization design of high-modulus supports under various load conditions, there are two control conditions: 1) the displacement of specified nodes must satisfy constraint conditions, and 2) the structural mass must be minimized. The mathematical model for the optimization problem is expressed as follows.

$$Findx = [x_1, x_2, \ldots, x_k]^T \tag{1}$$

$$minW = \sum_{e=1}^{n} L_e \rho_e A_e \tag{2}$$

$$u_{il} \leq u_i^*(i = 1,2,\ldots,m; l = 1,2,\ldots,p) \tag{3}$$

$$\underline{x}_j \leq x_j \leq \bar{x}_j(j = 1,2,\ldots,k) \tag{4}$$

Where: W is the mass of the structure; $u_{ij}$ is the displacement of node i under the l-th loading condition; $L_e$、$\rho_e$, and $A_e$ are the length, material density, and cross-sectional area of element e, respectively; n is the total number of bar elements in the structure; $u_i^*$ is the upper limit on the displacement of node i under all conditions; m is the total number of constrained node displacements; p is the number of loading conditions; k is the number of design variables; $\bar{x}_j$ and $\underline{x}_j$ are the upper and lower limits of the design for the j-th node coordinate $x_j$, respectively.

Assuming that the support is subjected to a set of external forces P and is in equilibrium, the use of finite element analysis ensures the continuity of truss structure deformation. The structural equilibrium equations and the overall stiffness matrix, in terms of the change in quantity $\Delta K$ relative to node j and the displacement $\Delta x_j$, can be linearly expressed as:

$$Ku = P \tag{5}$$

$$\Delta K = \sum_{e=1}^{n_j} \Delta\, k_e \approx \left( \sum_{e=1}^{n_j} \frac{\partial k_e}{\partial x_j} \right) \cdot \Delta x_j \tag{6}$$

In the equation: K is the overall stiffness matrix; $k_e$ is the element stiffness matrix; u is the column array of unknown node displacements; P is the column array of external loads. $n_j$ is the number of elements connected to the movable node j, and $n_j \ll$ n; $\Delta k_e$ is the change in the element stiffness matrix; $\Delta x_j$ is the displacement step size of node j to node.

It can be derived that the first derivative of the total stiffness matrix with respect to $x_j$ is equal to the sum of the first derivatives of the element stiffness matrices connected to node j. The formula is expressed as follows:

$$\frac{\partial K}{\partial x_j} = \lim_{\Delta x_j \to 0} \frac{\Delta K}{\Delta x_j} = \sum_{e=1}^{n_j} \frac{\partial k_e}{\partial x_j} \tag{7}$$

Taking the first derivative with respect to the design variable $x_j$ on both sides, we obtain the first derivative of the column array of node displacements with respect to the coordinate $x_j$, $\frac{\partial u}{\partial x_j}$, and simultaneously left multiply it by a unit virtual load array $F^{iT}$. The term corresponding to the displacement-constrained node i is equal to unity, while all other terms are zero. The derivative of node i's displacement can be expressed as:

$$F^{iT} \cdot \frac{\partial u_i}{\partial x_j} = -F^{i^T} K^{-1} \frac{\partial K}{\partial x_j} u = -(u^i)^T \frac{\partial K}{\partial x_j} u \tag{8}$$

In the equation, $u_i$ is the column array of node displacements caused by the unit virtual load $F^i$ acting independently on the structure, and it satisfies:

$$K u^i = F^i \tag{9}$$

Substituting equation (7) into equation (9), we can calculate the sensitivity of node i's displacement relative to the movement of node j as:

$$\frac{\partial u_i}{\partial x_j} = -\sum_{e=1}^{n_j} (u_e^i)^T \frac{\partial k_e}{\partial x_j} u_e \tag{10}$$

In the equation, $u_e^i$ and $u_e$ are the column arrays of node displacements caused by the unit virtual load and external load, respectively.

When performing the calculation, it is only necessary to consider the elements in the support structure that are related to node j, and the elements not connected to node j can be omitted. The change $\Delta u_{ij}$ in node i's displacement relative to the movement of node j can be approximated as:

$$\Delta u_{ij} \approx \frac{\partial u_i}{\partial x_j} \Delta x_j = -\left( \sum_{e=1}^{n_j} (u_e^i)^T \frac{\partial k_e}{\partial x_j} \right) \Delta x_j \tag{11}$$

The value of $\Delta u_{ij}$ can be either positive or negative, depending on the direction of movement for node j. To reduce the displacement $u_i$ of the specified node in the direction of its constrained value $u_i^*$, we have:

$$\Delta u_{ij} < 0 \ (j = 1,2, \dots k) \tag{12}$$

The direction of movement for node j is determined as follows:

$$sig(\Delta x_j) = sign\left(\sum_{\theta=1}^{n_j}(u_e^i)^T \frac{\partial k_e}{\partial x_j} u_e\right)(j = 1,2,\dots k) \quad (13)$$

The sig( ) in the equation represents the sign function. It can be seen that the direction of design variable search, i.e., the movement direction of node positions, is determined by sensitivity analysis.

***Cross-section variation optimization***

In the process of structural optimization design, it is necessary to calculate the response of the structure caused by external excitation. To assess the impact of design parameters on the structure's response, the problem involves solving the rate of change of structural response with respect to parameter variations. Taking the example of a plane bending beam element in the local coordinate system, the stiffness matrix is as follows:

$$k_e = \frac{El}{L^3}\begin{bmatrix} 12 & 6L & -12 & 6L \\ 6L & 4L^2 & -6L & 2L^2 \\ -12 & -6L & 12 & -6L \\ 6L & 2L^2 & -6L & 4L^2 \end{bmatrix} \quad (14)$$

In the calculation process, the plane beam element considers both axial deformation and bending deformation separately. The first-order derivative of the stiffness matrix for axial deformation is computed based on the stiffness matrix of the bar element, while the first-order derivative of the stiffness matrix for bending deformation is calculated using the minimum potential energy principle. From the stiffness matrix of the beam element, it is evident that the stiffness matrix of a pure bending beam element is proportional to the section's moment of inertia and does not include the cross-sectional area A. In most cases, the moment of inertia I of the beam section has a relationship with the cross-sectional area A and can be expressed using the following formula:

$$I = cx^s \quad (15)$$

Where c and s are constants determined by the section shape; x is the design variable.

In other words, when the cross-sectional area A is considered as the design variable, the first-order derivative of the stiffness matrix for the beam element with respect to A is：

$$\frac{\partial k_e}{\partial A} = \frac{\partial k_e^t}{\partial A} + \frac{\partial k_e^b}{\partial I}\cdot\frac{\partial I}{\partial A} = \frac{K_e^t}{A} + \frac{sK_e^b}{A} \quad (16)$$

In the equation, $k_e^t$ represents the stiffness matrix for the bar element, and $k_e^b$ represents the stiffness matrix for the bending element of the beam.

In the process of optimizing the lattice-type support structure, the cross-sectional area A can be decomposed into independent variables: diameter B and thickness T. The sensitivity of the diameter is the first-order derivative of the stiffness matrix for the beam element with respect to B, and the sensitivity of the thickness is the first-order derivative of the stiffness matrix for the beam element with respect to T. Diameter B and thickness T are not independent variables and can be converted to a general formula for differentiation with respect to the independent variable B or T.

In other words, when the beam cross-sectional diameter B is considered as the design variable, the first-order derivative of the stiffness matrix for the beam element with respect to B is:

$$\frac{\partial k_e}{\partial B} = \frac{\partial k_e^t}{\partial A}\cdot\frac{\partial A}{\partial B} + \frac{\partial k_e^b}{\partial B}\cdot\frac{\partial I}{\partial B} \quad (17)$$

The first-order derivative of the stiffness matrix of the beam element with respect to the thickness T of the beam section is given as follows:

$$\frac{\partial k_e}{\partial T} = \frac{\partial k_e^t}{\partial A}\cdot\frac{\partial A}{\partial T} + \frac{\partial k_e^b}{\partial T}\cdot\frac{\partial I}{\partial T} \quad (18)$$

## RESEARCH ON WIND-RESISTANT OPTIMIZATION DESIGN BASED ON THE OPTIMAL CRITERIA METHOD

### Parameter influence analysis

#### *Analysis of the impact of lattice-type high-modulus support steel pipe diameter on the structure*

In order to study the impact of lattice-type high-modulus support steel pipe diameter on the structure, it is assumed that the material of the lattice-type high-modulus support columns has a uniform cross-section and is homogeneous and elastic. Euler's critical load formula is used to calculate the critical load value.

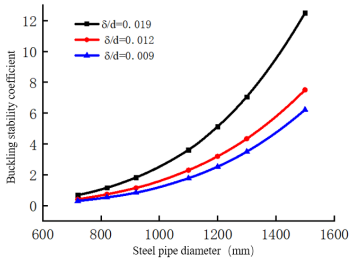


*Fig. 3 - Trend of buckling stability factor variation for steel pipe piles with non-proportional diameters.*

The ratio of steel pipe wall thickness δ to diameter d is an important control parameter for steel pipe manufacturing. Using this parameter, the critical buckling load factor for steel pipes of different diameters can be calculated. The relationship between the buckling stability factor and steel pipe diameter is shown in Figure 3-1.

From the analysis of the above figure, it can be inferred that when the ratio δ/d of steel pipes is the same, the critical buckling load factor of the structure is positively correlated with the steel pipe diameter, and the overall exponent continuously increases. When the steel pipe diameter remains unchanged and the wall thickness of the steel pipe is increased, the critical load factor of the structure increases with the increase of δ/d. This indicates that the cross-sectional dimensions of the support structure play a crucial role in its stability.

#### *The influence analysis of the number of columns in the lattice-type high-modulus support structure*

Reference to the Engineering Project, with Column Steel Pipe Diameters of Φ1200mm for Vertical Columns, Φ720mm for Horizontal Pipes, and Φ400mm for Diagonal Braces, for Further Investigation of the Relationship Between the Support Structure and the Number of Columns. By Establishing Finite Element Models for Single Columns, Double Columns, Four Columns, and Six Columns, the Critical Load Coefficient of the Support Structure is Calculated, as Detailed in Table 2 Below:

*Tab. 2 - Statistical data of different column numbers and critical load coefficients of support structures*

| Column numbers | Critical load coefficients | Model diagram | Remarks |
|---|---|---|---|
| Single column | 0.3009 | （a） | Single column |
| Double column | 0.3012 | （b） | Lateral spacing 9.0m |
| Four column | 10.830 | （c） | Lateral 9.0m, Along-Bridge 7.61m |
| Six Column | 10.890 | （d） | 2× Lateral 9.0m, Along-Bridge 7.61m |

The results of different column numbers in Figure 4 show that when the number of columns in the lattice-type support increases in the horizontal plane, it has a limited effect on the structural stability. However, when the number of columns in the vertical plane increases, the critical load coefficient grows rapidly, indicating improved stability and enhanced resistance to external loads. When transitioning to a spatial lattice-type support and increasing the number of columns to 6, the critical load coefficient does not change significantly. Therefore, considering stability and economic factors, it is optimal to choose 4 columns for the steel pipe lattice columns.

*Fig. 4 - Calculation results of models with different column numbers*

***Analysis of the impact of lattice-type high-modulus support spacing changes in the transverse and longitudinal directions***

The longitudinal and transverse spacing of lattice-type support columns is an important parameter for evaluating the stability of the support structure. To investigate the relationship between longitudinal and transverse spacing and the stability of the support structure, considering a segment length of 12 meters and an assembly height of 60 meters, we have recorded the numerical variations in different longitudinal and transverse spacings and critical load values as follows.

*Tab. 3 - Statistical table of different longitudinal and transverse spacing with critical load coefficients*

| Longitudinal and transverse arrangement | 5.0×5.0m | 6.0×6.0m | 7.0×7.0m | 8.0×8.0m | 9.0×9.0m | 10.0×10.0m |
|---|---|---|---|---|---|---|
| Critical load coefficient | 5.61 | 6.15 | 6.36 | 6.34 | 6.21 | 6.03 |

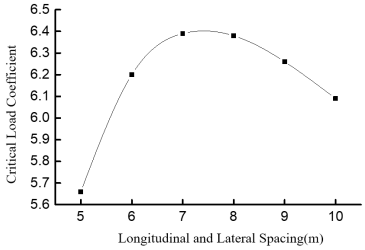


*Fig. 5 - Graph of longitudinal and transverse spacing of braces and critical load factor variations.*

The curve depicting the variation in longitudinal and transverse spacing and the critical load factor for grid-type braces exhibits a parabolic distribution. The spacing between braces falls within the range of 5-7m. The critical load factor increases with the widening of the brace spacing, reaching its peak at 7m. Between 7m and 10m, there is a decreasing trend in the critical load factor, indicating a decline in bracing stability. Notably, at a spacing of 8m, the critical load factor is slightly lower than at 7m, suggesting the possibility of the maximum critical load factor occurring within the range of 7m-8m. Therefore, for brace design, it is advisable to consider a spacing between 7m and 8m.

***Impact analysis of diagonal bracing in grid-formwork high-shoring structures***

The primary components of the grid-formwork high-scoring system include columns and horizontal struts. Diagonal bracing, serving as an auxiliary element, introduces certain effects.

Utilizing finite element analysis models for comparative analysis, the impact of diagonal bracing is assessed by contrasting the first three unstable modes.

For a grid-form column support system with diagonal bracing, the first-order critical load factor is 6.28, whereas without diagonal bracing, the factor reduces to 4.91. The second-order critical load factor is 6.46 with diagonal bracing and decreases to 5.18 without diagonal bracing. In the case of the third-order critical load factor, with diagonal bracing, it is 10.86, while without diagonal bracing, it reduces to 8.08. It is evident that the addition of diagonal bracing enhances the critical load factors of the support structure, resulting in an improvement ranging approximately between 25% and 35%. In structural design, diagonal bracing plays a crucial role.

**Optimal criterion modification**

Optimization is the process of simplifying a problem into a mathematical model that aligns with the practical loading conditions, and solving it through appropriate solution methods. Structural optimization requires determining three key aspects: 1) Independently varying optimization design variables; 2) An objective function concerning the design variables; 3) Constraint functions related to the feasible domain limits of the design variables.

$$\text{Design variables: } \{X\} = [X_1, X_2, \dots X_i, X_N]^T \tag{19}$$

$$\text{Objective function: } min\,imize\big(W(\{X\})\big) \tag{20}$$

$$\text{Constraint function: } \begin{matrix} f_k(\{X\}) = g_k(\{X\}) - g_k^U \le 0 (k = 1,2, \cdots m) \\ X_i^L \le X_i \le X_i^L \end{matrix} \tag{21}$$

In the equation: N is the total number of design variables $X_i$; m is the total number of constraint functions; $W(\{X\})$ is the expression of the objective function; $g_k^U$ is the limit value; $X_i^L$ and $\bar{X}_i^L$ are, respectively, the lower and upper limits of the design variable $\bar{X}_i^L$.

H.W. Kuhn and A.W. Tucker introduced the Kuhn-Tucker (K-T) conditions in 1951, which have become foundational in the field of nonlinear programming. The equation can be rewritten in the following form:

$$L(\{X\}, \lambda_k) = W(\{X\}) + \sum_{k=1}^{m} \lambda_k \left(g_k\{X\} - g_k^U\right) \tag{22}$$

Applying partial differentiation, the quadratic formula, and linear term simplification, we obtain:

$$X_i^{v+1} = X_i^v \left\{1 + \frac{1}{\eta}\left[\left(-\sum_{k=1}^{m} \lambda_k \frac{\delta g_k}{\delta X_i}\right) \Big/ \frac{\delta W}{\delta X_i} - 1\right]\right\}_v \tag{23}$$

In the equation, as the value of η increases, the differences in design variables decrease, controlled by dynamic changes to achieve convergence effects.Before obtaining the new design variables $X_i^{v+1}$, we first need to calculate the Lagrange multiplier $\lambda_k$. Considering the change in constraint functions $\left(g_k^{V+1} - g_k^v\right)$ due to variations in design variables $\left(X_i^{V+1} - X_i^v\right)$, this can be expressed as:

$$g_k^{V+1} - g_k^v = \sum_{i=1}^{N} \left(\frac{\delta g_k}{\delta X_i}\right)_v \left(X_i^{v+1} - X_i^v\right) \tag{24}$$

Considering that after the v+1 iteration, constraint k becomes an active constraint, i.e., we can derive a system of linear equations, expressed as follows:

$$\sum_{s=1}^{m}\lambda_s^v\sum_{i=1}^{N}\frac{\frac{\delta g_k}{\delta X_i}\frac{\delta g_s}{\delta X_i}}{\frac{\delta W}{\delta X_i}}X_i^v=-\sum_{i=1}^{N}\left(\frac{\delta g_k}{\delta X_i}\right)_v X_i^v-\eta(g_k^U-g_k^v) \tag{25}$$

When a value exceeds the predefined upper or lower limit for a variable, it is set equal to the upper or lower limit and remains unchanged within the current design cycle. At this point, the variable becomes inactive and remains unchanged in the next iteration when solving for $\lambda_s^v$

$$\sum_{s=1}^{m}\lambda_s^v\sum_{i=1}^{Na}\frac{\frac{\delta g_k}{\delta X_i}\frac{\delta g_s}{\delta X_i}}{\frac{\delta W}{\delta X_i}}X_i^v=-\sum_{i=1}^{Na}\left(\frac{\delta g_k}{\delta X_i}\right)_v X_i^v-\eta(g_k^U-g_k^v) \tag{26}$$

In the equation, $Na$ is the number of active variables. After obtaining the Lagrange multiplier $\{\lambda\}_{m\times1}$ and substituting it into the solution to get $X_i^{v+1}$, if $X_j^{v+1}$ exceeds the predefined limits of $X_j^U$ or $X_j^L$, it is set as $X_j^{v+1}$=$X_j^U$ or $X_j^{v+1}$=$X_j^L$, and the solution is carried out in the v+1 iteration.Therefore, when situation $X_j^{v+1}$>$X_j^U$ (or $X_j^{v+1}$<$X_j^L$) occurs in the current iteration, it is possible to modify the equation in the next iteration as the sum of active and inactive variables.

$$\begin{cases} g_k^{v+1}-g_k^v=\sum_{i=1}^{Na}\left(\frac{\delta g_k}{\delta X_i}\right)_v\left(X_i^{v+1}-X_i^v\right)+\sum_{j=1}^{Np}\left(\frac{\delta g_k}{\delta X_j}\right)_v\left(X_j^U-X_j^v\right), X_j^{v+1}\rangle X_j^U \\ g_k^{v+1}-g_k^v=\sum_{i=1}^{Na}\left(\frac{\delta g_k}{\delta X_i}\right)_v\left(X_i^{v+1}-X_i^v\right)+\sum_{j=1}^{Np}\left(\frac{\delta g_k}{\delta X_j}\right)_v\left(X_j^L-X_j^v\right), X_j^{v+1}\langle X_j^L \end{cases} \tag{27}$$

In the equation, $Np$ is the number of inactive variables in the current iteration. The stiffness matrix is modified as follows:

$$\begin{cases} \sum_{s=1}^{m}\lambda_s^v\sum_{i=1}^{Na}\frac{\frac{\delta g_k}{\delta X_i}\frac{\delta g_s}{\delta X_i}}{\frac{\delta W}{\delta X_i}}X_i^v=-\sum_{i=1}^{Na}\left(\frac{\delta g_k}{\delta X_i}\right)_v X_i^v-\eta(g_k^U-g_k^v)+\eta\sum_{i=j}^{Np}\left(\frac{\delta g_k}{\delta X_j}\right)_v\left(X_j^U-X_j^v\right), & X_j^{v+1}\rangle X_j^U \\ \sum_{s=1}^{m}\lambda_s^v\sum_{i=1}^{Na}\frac{\frac{\delta g_k}{\delta X_i}\frac{\delta g_s}{\delta X_i}}{\frac{\delta W}{\delta X_i}}X_i^v=-\sum_{i=1}^{Na}\left(\frac{\delta g_k}{\delta X_i}\right)_v X_i^v-\eta(g_k^U-g_k^v)+\eta\sum_{i=j}^{Np}\left(\frac{\delta g_k}{\delta X_j}\right)_v\left(X_j^L-X_j^v\right), & X_j^{v+1}\langle X_j^L \end{cases} \tag{28}$$

Therefore, when conducting the vv-th iteration of variable optimization using the optimal criterion method, if it is found that the results of the design variables in this iteration exceed the limit values, a new iteration is performed.

## Optimization of grid-formwork high-shoring against wind based on geometric nonlinear analysis

### *Optimization of mathematical computational models*

The objective of optimization is to minimize the weight of the grid-formwork high-shoring while meeting the requirements of various mechanical performances. Therefore, the mathematical model for the optimization of wind-resistant grid-formwork high-shoring structures based on geometric nonlinear analysis is as follows:

$$W=\sum_{i=1}^{N\theta}\gamma_i A_i l_i \tag{29}$$

Constraint conditions:

$$\begin{cases} \dfrac{u_{max}}{u^n} \\ \dfrac{\sigma_{max}}{\sigma^u} - 1 \le 0 \\ \dfrac{^c\lambda}{-5} \le -1 \end{cases} \tag{30}$$

In the equation, $^c\lambda$ is the critical load factor considering geometric nonlinear analysis, with a value of $^c\lambda$>5; displacement and stress constraints are set to the same limits as in linear analysis conditions.

Taking a four-legged grid-formwork high-shoring structure as a reference, the structural parameters are set as follows: the width of the shoring in the transverse bridge direction is determined to be 9m. The optimization variables include the thickness of the vertical strut T1, the thickness of the horizontal strut T2, the thickness of the diagonal strut T3, the width of the vertical strut in the along-bridge direction LL, and the diameters of the vertical B1, horizontal B2, and diagonal B3 struts—totaling 7 design variables. The initial design values are set as follows: T1=18 mm, T2=12 mm, T3= =10 mm, L=8000 mm, B1=1400 mm, B2=800 mm, B3=500 mm.

Displacement control follows the People's Republic of China's "Code for Design of Steel Structures" GB50017-2017 B.2, adopting the conservative value L/400. The safety factor for stress is set at 1.2, with a controlled stress of 179 MPa and a buckling coefficient control of 55. Using the ANSYS optimization calculation program with the OPT module, the structure is subjected to displacement, stress, structural stability, and volume sensitivity analyses. The main design variables influencing each control variable are determined, and significant adjustments are made to their design ranges. The sensitivity analysis is shown in Figure 6.

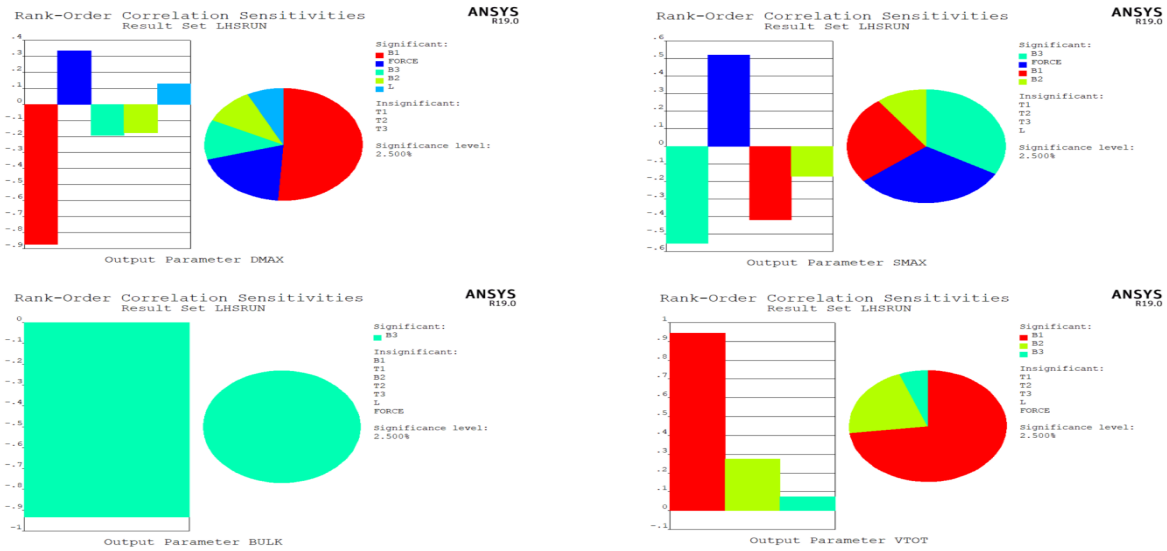


*Fig. 6 - Sensitivity analysis of the shoring structure*

Performing displacement, stress, structural stability, and volume sensitivity analyses on the model structure, as shown in Figure 5, reveals the following main design variables for each sensitivity: For displacement sensitivity, the primary design variable is the diameter of the vertical strut B1.For stress sensitivity, the primary design variable is the diameter of the diagonal strut B3.For overall stability sensitivity, the main design variable is the diameter of the diagonal strut B3.For overall volume stability sensitivity, the main design variable is the diameter of the diagonal strut B1.

Optimization objectives and constraint conditions must be defined numerically in the command flow so that they can be later read and called for algorithmic optimization. In APDL, extracting output results parameters (using the maximum displacement of the structure as an example) is done with the following command:

/POST1$DMAX=0$NSORT,U,Z$*GET,D_MAX,SORT,,MAX$*GET,D_MIN,SORT,,MAX$IF,ABS,(D_MAX),GT,ABS(D_MIN),THEN$DMAX=ABS(D_MAX)$ELSE$DMAX=ABS(D_MIN)$*ENDIF$PLNSOL,S,EQV,0$GET,EQVMAX,0,MAX

Based on the chosen constraint conditions, the wind-resistant optimization program calculations are conducted following the process outlined in Figure 6.

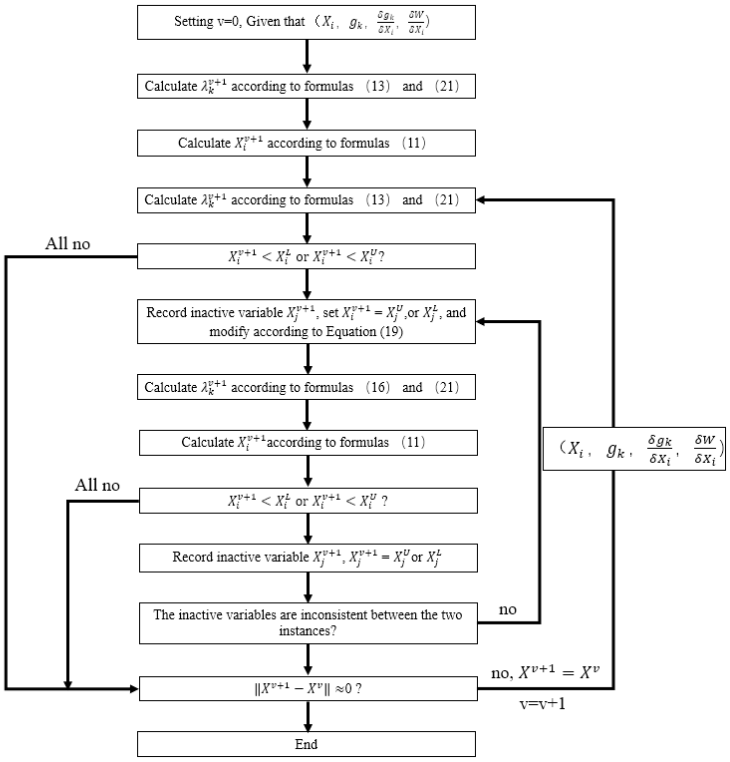


*Fig. 7- Modified flow chart of optimal criterion method*

***Optimization of Mathematical Computational Models***

(1) Iterative Results of Constraint Functions

Setting displacement and stress as constraint conditions, with a displacement constraint of 155mm and a stress constraint of 195MPa, plot the displacement response and the iterative representation of maximum equivalent stress as shown in Figures 8 and 9 after computational analysis.

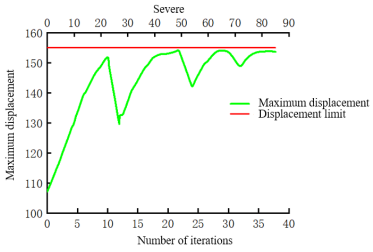


*Fig. 8 - Iterative results of maximum displacement response of the structure*

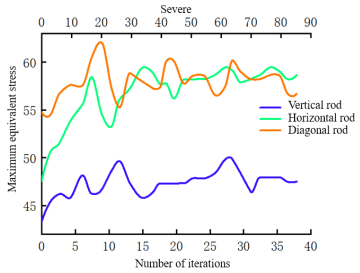


*Fig. 9 - Iterative results of the maximum equivalent stress of the structure*

(2) Iterative Results of Section Dimensions and Total Weight The iterative results of section dimensions and total weight are shown in Figures 10 and 11, respectively.

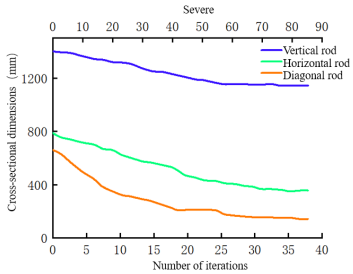


*Fig. 10 - Iteration results of section width of member*

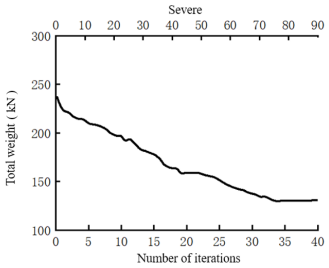


*Fig. 11 - The total weight of the structure is iterated*

Based on the analysis of the iterative curves above, the following conclusions can be drawn:

1) Geometric non-linear analysis is controlled by the top displacement constraint;
2) The maximum stress value occurs in the lower layer of the component's corner column;
3) The final section dimensions of the component decrease sequentially from the lower layer to the upper layer;
4) The curves exhibit good convergence;
5) Geometric non-linearity has an impact on the support structure.

***Critical Load Factor Constraint***

Setting the critical load factor as a constraint condition, with a constraint value of 5, perform computational analysis. Plot the iterative results of the structure's critical factor, section dimensions, and total weight, as shown in the respective figures.

(1) Iterative Results of Constraint Functions

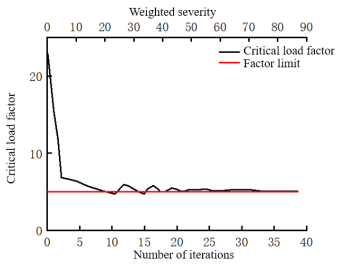


*Fig. 12 - Iterative results of critical load factor of structure*

(2) Iterative Results of Section Dimensions and Total Weight

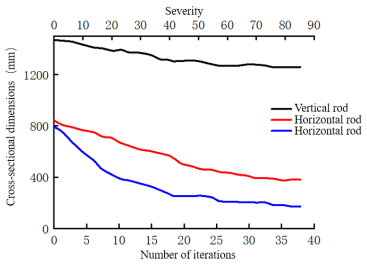


*Fig. 13 - Iteration results of section width of member*

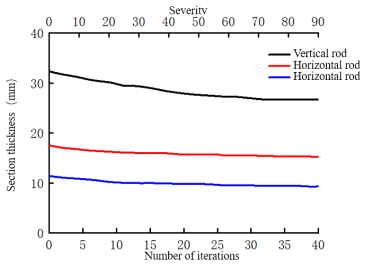


*Fig. 14 - Iterative results of section thickness of members*

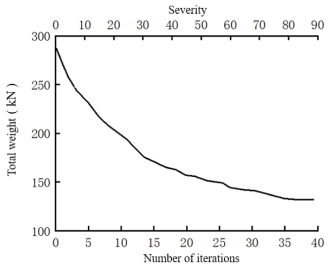


*Fig. 15 - The total weight of the structure is iterated*

From the analysis of the iterative curves above, the following results are obtained:

1. The critical load factor shows a good convergence in the inner loops, obtaining the corresponding limiting values.
2. The final section width of the components decreases sequentially from the bottom layer to the top layer.
3. All curves eventually converge.
4. The constraint conditions for the support structure are looser than those corresponding to the constraint conditions for the maximum structural displacement.

**Displacement, stress, and critical load factor as constraint conditions**

Setting displacement, stress, and critical load factor as constraint conditions with displacement constraint at 155mm, stress constraint at 195MPa, and critical load factor constraint at 5. After computational analysis, the iterative results of structural critical factor, maximum displacement response, section dimensions, and total weight are shown in Figures 16 to 21:

Iterative results of constraint functions.

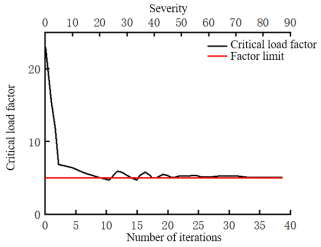


*Fig. 16 - Iterative results of structural critical load factor*


*Fig. 17 - Iterative results of maximum displacement response in the structure*

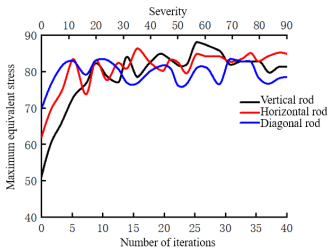


*Fig. 18 - Iterative results of maximum equivalent stress in the structure*

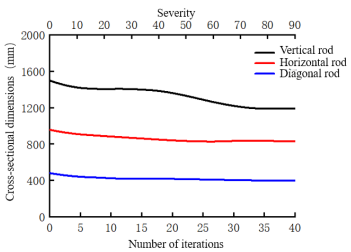


*Fig. 19 - Iterative results of component section width*

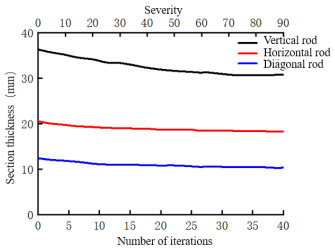


*Fig. 20 - Iterative results of component section thickness*

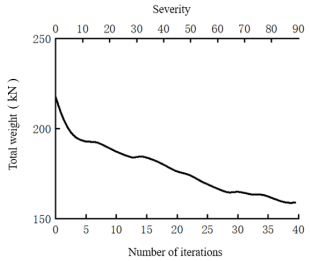


*Fig. 21 - Iterative results of structural total weight*

The results obtained from the above iterative curve analysis are as follows:

1) The support structure is controlled by the top displacement constraint;
2) The maximum stress value occurs in the lower layer of the component's corner column;
3) The final section dimensions of the component decrease sequentially from the lower layer to the upper layer;
4) All curves eventually converge.

## CONCLUSIONS

Based on finite element analysis using ANSYS, a simultaneous optimization of finite element models is conducted for four-leg and six-leg lattice-type supports, considering displacement deformation constraints and stiffness constraints. The study employs buckling stability coefficients and critical load factors to analyze the influence of steel tube diameter, the number of columns, longitudinal and transverse spacing of the support, and diagonal brace structural parameters on the structural stress performance. The optimal design process utilizes a modified optimal criterion method with relevant formulas, and a design flowchart is proposed for the wind-resistant optimization of lattice-type structures satisfying constraints such as stiffness, strength, and critical load factors.

Results obtained are as follows:

1. The iterative curves of constraint functions, section dimensions, and total weight exhibit good convergence under various conditions, indicating the feasibility of the proposed method;

2. When the ratio δ/d of column steel tubes is the same, there is a positive correlation between the structural critical buckling load factor and the steel tube diameter. The section dimensions of the support structure play a crucial role in its stability. The optimal number of columns for spatial lattice-type supports is four. The variation curve of longitudinal and transverse spacing of the lattice-type support and the critical load factor shows a parabolic distribution. Increasing diagonal braces enhances the critical load factor of the support structure;

3. In the optimization process of the lattice-type support structure, the main design variable for displacement sensitivity is the vertical rod diameter (B1); for stress sensitivity, it is the diagonal rod diameter (B3); for overall stability sensitivity, it is the diagonal rod diameter (B3); and for overall volume stability sensitivity, it is the diagonal rod diameter (B1). The set top displacement limit serves a controlling role, and the maximum stress value occurs in the lower-layer corner column.

According to this optimized design process, the multi-leg lattice-type high support structure meets all control values within the national safety standards during construction. This implies an improvement in economic efficiency while ensuring the rationality of the design.

This study will provide a favorable basis for the design of the construction system for future sea-crossing bridges in China. However, there is still room for improvement in the simulation technology of the structure. Further research is needed for the refinement of node finite element simulation and the multi-scale modeling of the overall-local structure.

## REFERENCES

[1] Wang Weixu, Wang Bin, Chen Cang, Yao Guanhua, & Huang Liang. 2022. Wind Resistance Analysis of Large Gantry Cranes for Bridge Construction. Highway (007), 067.
[2] Chen Zhaohui, Erik VanMarcke, Sun Yi, & Li Zhengliang. 2008. Review of Extreme Wind Speed Prediction Models for Conventional Wind and Hurricanes. Journal of Natural Disasters, 17(5), 6.
[3] Shen Ke liang. 2023. Analysis of the Construction Technology of Full-support Formwork in Bridge Engineering. Development Guidance of Building Materials (020), 021.
[4] Zhang Zhen. 2023. Application of Single-span Double-layer Bailey Beam Bracket in Cast-in-place Construction of High-pier Bridges. Anhui Architecture.
[5] Wang Shijie. 2021. Study on Wind-induced Response of Lattice-type High Pile in Typhoon-prone Area for Sea-crossing Bridges. (Doctoral dissertation, Northeast Forestry University).
[6] Zhang Yang, & Wang Xiaojing. 2018. Overall Stability Analysis and Design Suggestions for Lattice-type Support. Northern Traffic, (11), 4.
[7] Jiang Yue. 2020 Research on stability bearing capacity of steel column-beams supporting system. (Guilin university of technology).
[8] Law, S. S. , Bu, J. Q. , & Zhu, X. Q. . 2005. Time-varying wind load identification from structural responses. Engineering Structures, 27 (10), 1586-1598.
[9] Li Feng, Zou Lianghao, Liang Shuguo, Chen Yin. 2020. Spatial Correlation Study of Lateral Fluctuating Wind Loads on Grid Structure Tower. Journal of Vibration and Shock, 39(5), 7.
[10] Du Hang, Xu Haiwei, Zhang Yuelong, & Lou Wenjuan. 2022. Wind Pressure Characteristics and Wind-induced Vibration Response of Large-span Flexible Photovoltaic Support Structure. Journal of Harbin Institute of Technology (010), 054.
[11] Guan Xian, & Tang Guohua. 2022. Study on the Mechanical Behavior of Suspended Scaffold Method in the Construction of Reinforced Concrete Composite Beams. Highway Traffic Science and Technology, 39(10), 84-90.
[12] Hwang, J. S. , Kareem, A. , & Kim, H. .2011. Wind load identification using wind tunnel test data by inverse analysis. Journal of Wind Engineering & Industrial Aerodynamics, 99(1), 18-26.
[13] Tan Wenshu. 2017. Research on Wind-resistant Optimization Method of Lattice Tall Structure Based on Genetic Algorithm and Critical Load Factor. (Doctoral dissertation, Guangzhou University).
[14] Yu Xiulei, Liang Shuguo, & Zou Lianghao. 2006. Simplified Calculation of Downwind Wind-induced Vibration Response of Lattice Tower. Journal of Huazhong University of Science and Technology: Urban Science Edition (z2), 3.
[15] Wen Yang, Yu Jiao, & Meng Chunnan. 2022. Study on the Yield Mechanism of the Encased Spherical Plate Branch Node in the Lattice Steel-Concrete Wind Power Generation Tower. Journal of Chongqing University (005), 045.
[16] B. A J ,Ziad A & Abdollah S , et al. 2023 Revisit of underestimated wind drag coefficients and gust response factors of lattice transmission towers based on aeroelastic wind tunnel testing and multi-sensor data fusion. Engineering Structures,278.
[17] Fan Xinliang, & Wang Tong. 2021. Implementation of Finite Element Model Modification Software Based on ANSYS. Mechanical Manufacturing and Automation, 50(1), 4.
[18] Zhou Peng. 2023. Euler Formula Analysis of Critical Force for Local Reinforcement of Tower Components. China Building Metal Structure, 22(3), 86-88.